Spatially resolved *in situ* measurements of the transport of organic molecules in a polycrystalline nanoporous membrane

Weontae Oh[a] and Sankar Nair[b]
School of Chemical & Biomolecular Engineering, Georgia Institute of Technology, 311 Ferst Drive NW, Atlanta, Georgia 30332-0100

(Received 25 April 2005; accepted 18 August 2005; published online 7 October 2005)

We report spatially resolved, quantitative, *in situ*, nondestructive measurements of the transport of organic molecules through a polycrystalline, anisotropic, nanoporous molecular sieve membrane, with micron-scale resolution. A method based on photoacoustic spectroscopy experiments during permeation through a nanoporous membrane, combined with a physical model of photoacoustic signal generation from a heterogeneous membrane, allows extraction of concentration profiles *in situ*. In particular, we demonstrate the steady-state concentration profiling of the organic molecules *p*-xylene and *n*-hexane during their transport through a nanoporous zeolite silicalite membrane. The implications for elucidating structure-property relationships in membrane materials for separations, catalytic, or nanotechnology applications are discussed. © *2005 American Institute of Physics*. [DOI: 10.1063/1.2093918]

Nanoporous polycrystalline membranes, made from materials such as zeolites or mixed oxides are being investigated extensively[1–4] for technological applications in separations, catalysis, and as ordered hosts for arrays of nanomaterials such as nanowires, nanoclusters, and nanotubes. Their attractiveness is due to the existence of a well defined, periodic nanopore structure.[2,3] Unambiguous measurements and theoretical descriptions of molecular transport in these tightly confined nanoporous environments, remain critical issues in advancing the application of these membranes.[5–12] The main experimental difficulty[6] has been to obtain *in situ*, quantitative, nondestructive, spatially resolved measurements of guest species concentrations with micron or submicron resolution over length scales of several tens of microns. This capability would constitute a powerful way of studying membrane transport, providing a completely transport-model-independent characterization that can be used to directly test detailed transport models.[6,9–12] In this letter, we present spatially resolved, *in situ* measurements of diffusing molecule concentration profiles through a nanoporous zeolite membrane. This is accomplished via: (1) design of an *in situ* photoacoustic sample cell that allows simultaneous membrane permeation and spectroscopic experiments, and (2) an experimentally validated physical model to analyze the data and extract the concentration profiles.

In step scan photoacoustic spectroscopy (SSPAS),[13–17] an IR beam modulated at a chosen frequency (5–1000 Hz) is absorbed by the sample and converted into a thermoacoustic signal originating from a cumulative region of the sample down to a certain depth μ (called the sampling depth). The acoustic signal is detected by a sensitive microphone and transformed to an IR spectrum as shown in Fig. 1. The use of a step scan interferometer provides the same sampling depth over the entire spectral range. Like conventional Fourier-transform IR (FTIR), SSPAS is very sensitive to the vibrational properties of the sample. However, it is applicable for highly absorbing samples, since the acoustic signal strength increases with the optical absorption strength of the material. In this letter we also present a simple physical model for obtaining concentration profiles from films containing a continuously varying concentration of guest molecules. To provide an initial validation of the model, a two-layer membrane was constructed by growing a zeolite membrane layer on alumina, calcining it to remove the organic structure directing agent (SDA), and then growing a second layer on the first. The resulting step-function SDA concentration profile[17,18] is well reproduced (Fig. 2) using the measurement model described later. The situation of physical interest is then described, namely demonstration of *in situ* concentration profiling of organic molecules transported across the membrane at steady state.

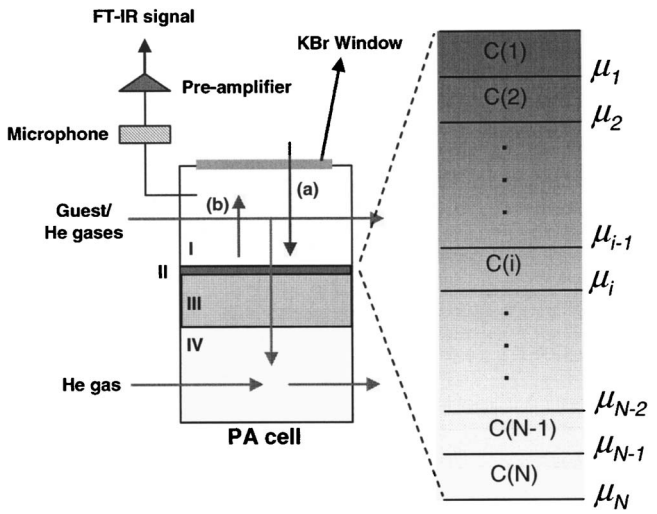

FIG. 1. Schematic of SSPAS experiment: (a) frequency-modulated incident IR signal, (b) generated acoustic signal. Region (I) feed side: a guest species vapor mixed with He carrier gas, (II) calcined silicalite membrane, (III) macroporous α-alumina substrate, and (IV) sweep side: pure He gas enters and sweeps out the guest species permeant. For mathematical analysis, the membrane was divided into N sublayers, wherein $C(i)$ is the guest concentration in sublayer i, and μ is the sampling depth.

[a]Current address: Department of Information Materials Engineering, Dongeui University, 955 Eomgwangno, Busanjin-gu, Busan 614–714, Republic of Korea.
[b]Electronic mail: sankar.nair@chbe.gatech.edu

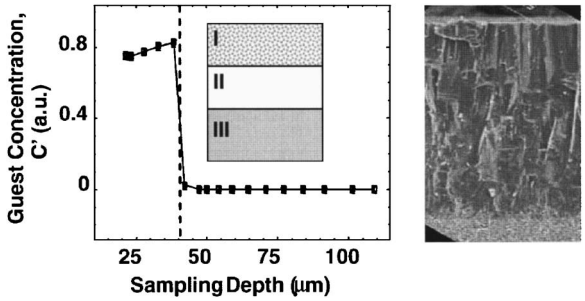

FIG. 2. Step-function concentration profile of tetrapropylammonium ions in a double-layered silicalite membrane (the cross-sectioned SEM image is shown in the right side) determined by SSPAS using Eq. (4). The membrane is composed of an upper layer (I) with uniformly-distributed TPA and a lower layer (II) without TPA on a substrate (III).

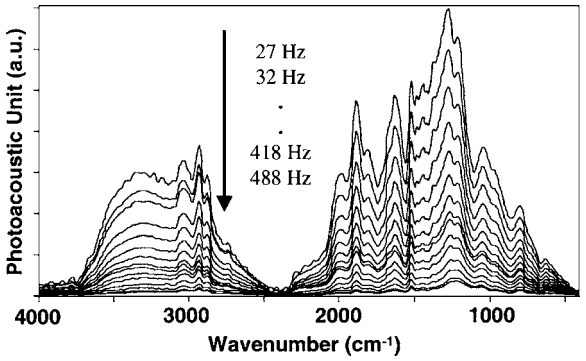

FIG. 3. SSPAS spectra measured *in situ* during steady-state permeation of *p*-xylene through the silicalite membrane, at increasing values of modulation frequency (and, hence, decreasing sampling depths).

A 100 μm, highly oriented (along the crystal c direction) silicalite zeolite membrane was hydrothermally grown on a macroporous α-alumina substrate[16] and was calcined to remove the tetrapropylammonium SDA. This nanoporous film is used for single-component permeation of *p*-xylene or *n*-hexane, employing the apparatus in Fig. 1. A sample cell that allows simultaneous permeation and photoacoustic spectroscopy experiments has been developed. The membrane is sealed between two small chambers through which a gas or vapor can be circulated. Helium (He, 99.9995%) is used as a carrier for the organic guest molecules. An organic/He stream is circulated in the upper chamber, whereas pure He is circulated in the lower chamber to sweep away the permeating organic molecules. The partial pressure (P/P_{sat}) of a guest molecule vapor was adjusted by combination of a saturated organic/He stream with the pure He diluent. SSPAS experiments were carried out on an IFS-55 FTIR spectrometer (Bruker) with an MTEC 300 photoacoustic detection module. The reference spectra (using carbon black as reference) were collected at the same vapor partial pressures in which sample spectrum was obtained. The spectra were collected over 4000–400 cm^{-1} with a resolution of 8 cm^{-1} and double-sided interferograms. Modulation frequencies were chosen in the range 16–488 Hz and with an amplitude of $4\lambda_{\text{HeNe}}$. After the SSPAS experiments, the membrane was cross sectioned and imaged by field-emission scanning electron microscopy (SEM) (Hitachi S800, 10 kV).

When the permeant is heterogeneously distributed at steady state in the film, the photoacoustic signal intensity $Q(\mu)$ for a particular sampling depth μ is expressed as

$$Q(\mu) = K\int_0^{\mu} [\beta_0 + \beta_1 C(x)] \times \exp\{-[\beta_0 + \beta_1 C(x) + \mu^{-1}]x\}dx, \tag{1}$$

where K is a system-dependent constant, β_0 is the optical absorption coefficient of the host membrane, β_1 is the optical absorption coefficient per unit concentration of the guest species for a guest-templated zeolite membrane, and μ the thermal diffusion length,[13] which is given byg modulation frequency, f of the step scan interferometer. Since the membrane is optically transparent and thermally thick (i.e., the sampling depth is much smaller than the optical absorption length of the material),[13,14] Eq. (1) reduces to

$$Q \cong K\beta_0\int_0^{\mu} e^{-x/\mu}dx + K\beta_1\int_0^{\mu} C(x)e^{-x/\mu}dx. \tag{2}$$

To simplify Eq. (2), the membrane with a continuously varying distribution of guest species is discretized into N sublayers, within which the guest concentration, $C(i)$ is uniform (Fig. 1). This is a laterally averaged concentration over the sublayer, thus averaging out possible inhomogeneities in the concentration between different grains in the polycrystalline film. If the sampling depth $\mu=\mu_n$ extends to n layers, then Eq. (2) is discretized to

$$Q(\mu_n) \cong K\beta_0\mu_n(1-1/e) + K\beta_1\sum_{i=1}^{n} C(i)\mu_n(e^{-\mu_{i-1}/\mu_n} - e^{-\mu_i/\mu_n}). \tag{3}$$

Here the first term is the contribution from the membrane and the second term from the guest distribution. For a particular sampling depth μ_i, therefore, the signal intensity ratio of guest (g) species to zeolite membrane (m), Q_g/Q_m, is given by

$$\left(\frac{Q_g}{Q_m}\right)_i = \left(\frac{\beta_1}{\beta_0}\right)\frac{\sum_{k=1}^{i} C(k)(e^{-\mu_{k-1}/\mu_i} - e^{-\mu_k/\mu_i})}{(1-1/e)}. \tag{4}$$

Equation (4) is obtained by using the fact that the concentration of the zeolite remains constant over the film thickness. $C(k)$ is the depth-dependent concentration of the guest species in kth sublayer. We obtain a dimensionless concentration in each sublayer, $C'(k)=(\beta_1/\beta_0)C(k)$, by measuring SSPAS spectra at progressively increasing sampling depths. A series of spectra are measured (Fig. 3), each at a different sampling depth. The left-hand side of Eq. (4) is obtained as the ratio of integrated intensities of the characteristic bands of the guest species and the host zeolite, using the SSPAS spectrum corresponding to each sampling depth. This procedure for a given SSPAS spectrum, has been described by us in detail previously.[17] At the smallest μ, only one term, $C'(1)$, appears on the right-hand side of Eq. (4). $C'(1)$ can thus be measured, and its value is used to determine $C'(2)$ from the next measurement at an incrementally larger μ. This procedure is iterated until the silicalite-alumina interface is reached. For the membrane with the step-function concentration, the above method reproduces the shape of the tetrapropylammonium (TPA) SDA profile (Fig. 2). The slight decrease of TPA concentration near the surface in the upper

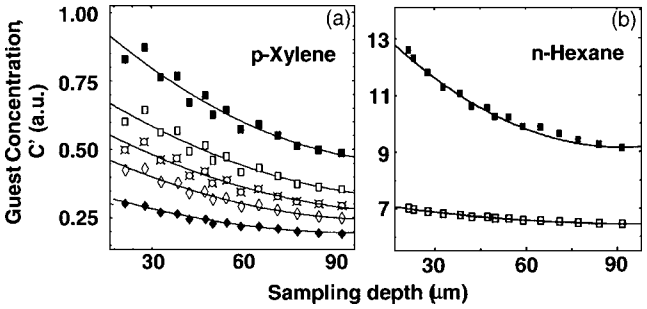

FIG. 4. (a) Experimental concentration profiles of *p*-xylene guest molecules permeating in a silicalite zeolite membrane at feed partial pressures P/P_{sat} of 1.00 (■), 0.86 (□), 0.71 (○), 0.50 (◇), and 0.29 (◆). (b) Experimental concentration profiles of *n*-hexane permeating in a silicalite zeolite membrane at feed partial pressures P/P_{sat} of 0.29 (■) and 0.14 (□). The error bars are smaller than the symbol sizes. The continuous curves are only a guide for the eye.

layer is caused by surface roughness effects, which decrease the signal-to-noise ratio at small sampling depths. These effects are damped out as the sampling depth is increased.

Figures 4(a) and 4(b) show the experimentally measured concentration profiles in a nanoporous molecular sieving membrane. Figure 4(a) shows the steady-state *p*-xylene profiles at 25 °C, with different feed partial pressures (P/P_{sat}) of *p*-xylene between 0.29 and 1.00. The spectral peaks of *p*-xylene and the zeolite are assigned according to previous literature[19,20] before spectral analysis was carried out. The integrated intensities of the 2879, 2936, and 3023 cm^{-1} (*p*-xylene) and 790 cm^{-1} (zeolite) were used for the quantitative analysis. The concentration of *p*-xylene gradually decreases over the depth of 100 μm. As P/P_{sat} increases, the entire profile shifts upward. The concentrations at the feed and permeate sides both increase, due to the increased chemical potential of the organic vapor on the feed side as well as insufficient removal of the permeant by the sweep gas on the permeate side. This suggests a significant transport resistance not only in the membrane but also at the interface of the membrane and the substrate.[21] By increasing the sweep flow from 3.3 to 120 mL/min, the measured concentration of *p*-xylene at the permeate side became negligible. Thus the technique can provide detailed information on the relative contributions of transport resistances in the membrane, the interface, and the substrate. Concentration profiles of *n*-hexane for two values of feed partial pressures are shown in Fig. 4(b). The characteristic SSPAS bands of *n*-hexane are assigned to 1385, 1467, 2878, 2937, and 2965 cm^{-1}. The signal intensities of the 1385 and 1467 cm^{-1} bands were used for quantitative analysis. The signal strength is an order of magnitude larger than for *p*-xylene, due to the larger number of C–H bonds (used as the characteristic bands) in *n*-hexane as well as its higher concentration in the membrane. In both cases, the concentration profiles are significantly nonlinear, implying that the diffusion coefficients are concentration dependent. Since the sampling depth can be set to a value exceeding the membrane thickness, the method described here can also be used for measuring the overall adsorption of molecules in the nanoporous host membrane. Such measurements are difficult to perform by conventional gravimetric or spectroscopic techniques, considering the small membrane mass (in relation to the substrate) and its optical absorption.

In conclusion, we have demonstrated a method for studying membrane transport based upon direct *in situ* measurement of concentration profiles with micron-scale resolution under actual transport conditions. The apparatus can be easily attached to a gas chromatograph to analyze the permeate stream, so that the transmembrane flux (J) (Refs. 5 and 6) can be measured. Hence, important quantities such as the concentration-dependent diffusivity of a permeant in the nanoporous membrane can be measured directly as $D(C) = -J/(\partial C/\partial x)$. The determination of $D(C)$ has been the subject of extensive theoretical and simulation efforts.[6–10] Additionally, measurements on oriented membranes will yield information on anisotropic diffusion, which was not possible with nuclear magnetic resonance and neutron scattering measurements on powder samples. Our method is also applicable to mixtures for which a distinguishable IR band for each of the guest species can be identified. In our view, the development described here has important implications for the current efforts towards understanding transport in nanoporous materials and membranes.

The authors acknowledge financial support from the Georgia Institute of Technology (start-up funding) and the National Science Foundation (CTS-0437621).

[1] Z. Lai, G. Bonilla, I. Diaz, J. G. Nery, K. Sujaoti, M. A. Amat, E. Kokkoli, O. Terasaki, R. W. Thompson, M. Tsapatsis, and D. G. Vlachos, Science **300**, 456 (2003).
[2] M. E. Davis, Nature (London) **417**, 813 (2002).
[3] M. Tsapatsis, AIChE J. **48**, 654 (2002).
[4] W. H. Yuan, Y. S. Lin, and Y. S. Yang, J. Am. Chem. Soc. **126**, 4776 (2004).
[5] S. Nair, M. Tsapatsis, in *Handbook of Zeolite Science and Technology*, edited by S. M. Auerbach, K. A. Carrado, and P. K. Dutta (Marcel Dekker, New York, 2003), p. 867.
[6] J. Kärger, S. Vasenkov, and S. M. Auerbach, in *Handbook of Zeolite Science and Technology*, edited by S. M. Auerbach, K. A. Carrado, P. K. Dutta (Marcel Dekker, New York, 2003), p. 341.
[7] T. C. Bowen, R. D. Noble, and J. L. Falconer, J. Membr. Sci. **245**, 1 (2004).
[8] C. Blanco and S. M. Auerbach, J. Am. Chem. Soc. **124**, 6250 (2002).
[9] D. Paschek and R. Krishna, Langmuir **17**, 247 (2001).
[10] A. I. Skoulidas and D. S. Sholl, J. Phys. Chem. A **107**, 10132 (2003).
[11] A. I. Skoulidas, D. S. Sholl, and R. Krishna, Langmuir **19**, 7977 (2003).
[12] A. I. Skoulidas and D. S. Sholl, AIChE J. **51**, 867 (2005).
[13] A. Rosencwaig and A. Gersho, J. Appl. Phys. **47**, 64 (1976).
[14] E. Y. Jiang, Spectroscopy **17**, 22 (2002).
[15] A. Rosencwaig and A. Gersho, Science **190**, 556 (1975).
[16] L. Gonon, J. Mallegol, S. Commereuc, and V. Verney, Vib. Spectrosc. **26**, 43 (2001).
[17] W. Oh and S. Nair, J. Phys. Chem. B **108**, 8766 (2004).
[18] G. Xomeritakis and M. Tsapatsis, Chem. Mater. **11**, 875 (1999).
[19] E. R. Geus, J. C. Jansen, and H. van Bekkum, Zeolites **14**, 82 (1994).
[20] Y. S. Lin, N. Yamamoto, T. Yamaguchi, T. Okubo, and S.-I. Nakao, Microporous Mesoporous Mater. **38**, 207 (2000).
[21] D. A. Newsome and D. S. Sholl, J. Phys. Chem. B **109**, 7237 (2005).